Rocket Plume Impingement Heat Transfer on Plane Surfaces

E. Mayer* and R. Prickett†
Hughes Aircraft Company, El Segundo, California

An analytic procedure has been derived for the rapid calculation of maximum heat flux on a flat plate due to the impingement of liquid rocket exhaust plumes. The impingement configurations considered generally lead to plume flow in the transitional flow regime, described in the approximation of a source flow expression. Newtonian impact analysis is employed to determine the location of the maximum pressure, considered to result in a stagnation point within the Newtonian shock layer. The Detra and Hidalgo atmospheric re-entry heat-transfer equation is modified to account for the effects of oblique plume flow incidence and related asymmetric shock-layer flow in the neighborhood of the stagnation point. The modified re-entry heating expression, including a single correlation factor of the order of unity, is shown to agree with extensive test data available on liquid-bipropellant heat transfer reported by Piesik et al. The analytical procedure yields improved correlation of the peak heat-transfer data and, because of its flexibility in predicting data trends with configuration changes, proves to be useful in the preliminary design of rocket reaction control systems.

Nomenclature

c^*	= characteristic velocity
C_F	= thrust coefficient
$C_{F,i}$	= ideal limit thrust coefficient
E^2	= percent error squared
F	= thrust
g	= gravity acceleration
h	= distance from nozzle exit center to plate centerline, defined in Fig. 2
I_{sp}	= specific impulse
$I_{sp,i}$	= ideal vacuum specific impulse
K	= correlation constant
p	= pressure
p_m	= maximum Newtonian impact pressure
p_s	= pressure behind shock
q	= heat flux
Q_m	= heat flux Kq_m defined analytically; independent of K
q_m	= calculated maximum heat flux
q_{max}	= measured maximum heat flux
q_N	= stagnation point heat flux in atmospheric re-entry, Eq. (19)
r	= radial distance from nozzle exit center
R_b	= effective blunt body radius correlated to R_p
R_e	= nozzle exit radius
R_p	= effective stagnation zone radius on plate
R_t	= nozzle throat radius
R_N	= spherical nose radius in atmospheric re-entry, Eq. (19)
T_g	= gas stagnation temperature
T_i	= initial temperature of re-entry body or flat plate
u	= velocity in Newtonian shock layer
V_∞	= maximum velocity in fully expanded plume
$\dot{W}$	= mass flow rate
x	= coordinate along plume axis
x'	= coordinate along surface
α,β	= source flow parameters defined in Eqs. (3) and (4)
γ	= specific heat ratio
δ	= plate cant angle
ϵ	= nozzle area expansion ratio
θ	= flow angle referred to plume axis
θ_e	= nozzle exit angle
θ_m	= flow angle of maximum Newtonian impact pressure
ρ	= plume density
ρ_m	= gas density in shock layer
ρ_{SL}	= sea level density of air

Presented as Paper 86-1321 at the AIAA/ASME 4th Joint Thermophysics and Heat Transfer Conference, Boston, MA, June 2–4, 1986; received June 13, 1986; revision received Sept. 22, 1986.

*Senior Scientist, Propulsion Department, Space and Communications Group. Member AIAA.

†Staff Engineer, Propulsion Department, Space and Communications Group. Member AIAA.

I. Introduction

IN spacecraft design, it is often necessary to evaluate the heating effect of rocket plume impingement on adjacent structures downsteam of the nozzle exit. Under these conditions, plume impingement occurs generally in the transitional flow regime, as contrasted with free molecule impingement conditions obtained in the highly rarefied regions of the plume. In the transitional regime, only limited representative test data[1,2] are available for generating useful correlations. Attempts at theoretical modeling of the complex gasdynamic effects in the transitional regime of plume impingement (e.g., Refs. 1-3) have had limited success in accounting for the available test data.

The objective of the present investigation is to develop an analytic procedure for calculating the maximum heat flux and its location when the plume impinges on a plane surface. The analytic procedure is intended both to enable rapid approximate calculations useful in the preliminary design of liquid-propellant reaction control systems and to provide insight into data trends with changing configuration parameters. Accordingly, a simplified description of the plume, previously successfully applied to drag effects in the transitional flow regime,[4] is given in Sec. II. Maximum heat flux is considered to occur where the impingement pressure, as calculated in Sec. III by Newtonian impact analysis, is a maximum. Heat flux at the peak pressure point is then calculated in Sec. IV by an elementary modification of a semiempirical expression for transitional flow heat transfer in atmospheric re-entry.[5]

Comparison of the calculated values with the liquid-propellant test data of Ref. 1, detailed in Sec. V, shows satisfactory overall agreement upon use of a correlation factor of the order of unity. A discussion of the results, including comments on the (aluminized) solid-propellant data of Ref. 2, is given in the concluding remarks of Sec. VI.

II. Plume Flowfield Simplified Description

A source flow method[4] is employed for simplified description of the plume flowfield. In the polar coordinate system (r,θ), shown in Fig. 1, the plume density $\rho(r,\theta)$ is assumed to have a three-parameter $(\alpha, \beta, V_\infty)$ form of the source flow,

$$\rho(r,\theta) = \frac{\alpha[\cos(\theta/2)]^\beta}{V_\infty r^2} \tag{1}$$

where V_∞ is the maximum velocity, directed along r, attained "far" from the source. This parameter is, in principle, related to the maximum "ideal" specific impulse $I_{sp,i}$, obtainable upon expansion of the rocket exhaust products to vacuum,

$$V_\infty = gI_{sp,i} \tag{2}$$

The other parameters, calculated by mass and momentum conservation laws, are related to total mass flow rate $\dot{W}$ and rocket thrust F as derived in the Appendix,

$$\dot{W} = \frac{8\pi\alpha}{\beta+2} \tag{3}$$

$$F = \frac{\beta}{\beta+4}\dot{W}\frac{V_\infty}{g} \tag{4}$$

In an alternative form,[4] β can be calculated from supersonic exit nozzle parameters, such as the area expansion ratio ϵ, exit angle θ_e, and gas specific heat ratio γ. The latter form is conveniently expressed in the ratio of thrust coefficient C_F to its ideal limit value $C_{F,i}$,

$$\frac{\beta}{\beta+4} = \frac{C_F}{C_{F,i}} \tag{5}$$

where analysis[6] yields

$$C_{F,i} = \sqrt{\frac{2\gamma^2}{\gamma-1}\left(\frac{2}{\gamma+1}\right)^{(\gamma+1)/(\gamma-1)}} \tag{6}$$

and

$$\frac{C_F}{C_{F,i}} = \frac{1+\cos\theta_e}{2}\sqrt{1-\left(\frac{p_e}{p_0}\right)^{(\gamma-1)/\gamma}} + \frac{p_e\epsilon}{p_0 C_{F,i}} \tag{7}$$

with p_e/p_0 representing the ratio of exit to chamber pressure, obtainable for given ϵ and γ from gasdynamic relations.

The preceding expressions refer to analytic results for ideal inviscid nozzle flow and will be used in the treatment of the data of Ref. 1. This is plausible because the peak heating effects arise by impingement of the inviscid portion of the nozzle (core) flow. It is noted that, for nonideal nozzle flows, β can be calculated from Eq. (5) if test data on C_F are available, since this parameter contains, implicitly, the effects of nozzle area expansion ratio, exit angle, viscous flow, heat losses, and all influences that reduce C_F below the ideal value $C_{F,i}$. Another propulsion parameter is the combustion efficiency, inferred from test data on c^* efficiency,[6] which must be considered in the evaluation of V_∞ from thermal energy data. Finally, it is noted here that the use of source flow formulas is usually limited to "far-field" applications. Nevertheless, as shown below, the application of Eq. (1) to the transitional flow data of Ref. 1 leads to satisfactory agreement with the heat-transfer test data of Ref. 1.

III. Newtonian Impact Pressure

For the purpose of calculating the maximum impingement pressure, we apply Newtonian impact concepts to the flow configuration shown in Fig. 2. In this figure, the impingement is symmetric about the plane of the figure, which shows the projection of the target plane TT parallel to the plume axis at a distance h from the axis. The impingement point on TT in the plane of symmetry is defined by the coordinate θ with $r = h/\sin\theta$. The impact pressure along TT given by the Newtonian "square law"[7] is

$$p_s(\theta) = \rho(\theta) V_\infty^2 \sin^2\theta \tag{8}$$

where, in view of Eqs. (1) and (3), the impingement plume density can be replaced by

$$\rho(r,\theta) = \rho(\theta) = \left(\frac{\beta+2}{8\pi}\right)\frac{\dot{W}}{V_\infty h^2}\sin^2\theta\left(\cos\frac{\theta}{2}\right)^\beta \tag{9}$$

With Eq. (9) used in Eq. (8), the pressure $p_s(\theta)$ is expressible as

$$p_s(\theta) = \text{const}\ \sin^4\theta\left(\cos\frac{\theta}{2}\right)^\beta \tag{10}$$

which becomes a maximum at $\theta = \theta_m$, obtainable from

$$\tan\theta_m \tan\frac{\theta_m}{2} = \frac{8}{\beta} \tag{11}$$

so that the maximum impact pressure $p_m = p_s(\theta_m)$.

A generalization of Eq. (11) to include the effect of plane cant angle δ leads to

$$\tan(\theta_m - \delta)\tan\frac{\theta_m}{2} = \frac{8}{\beta} \tag{12}$$

When the angle δ is produced by canting as shown in the dotted trace of the target plane T′T′ in Fig. 2, the impingement coordinate $r_m = r(\theta_m)$ is obtained as

$$r_m = \frac{h\cos\delta}{\sin(\theta_m - \delta)} \tag{13}$$

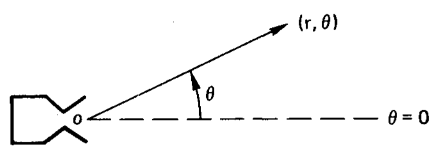

Fig. 1 Polar coordinate system (r,θ) with origin O at nozzle exit center.

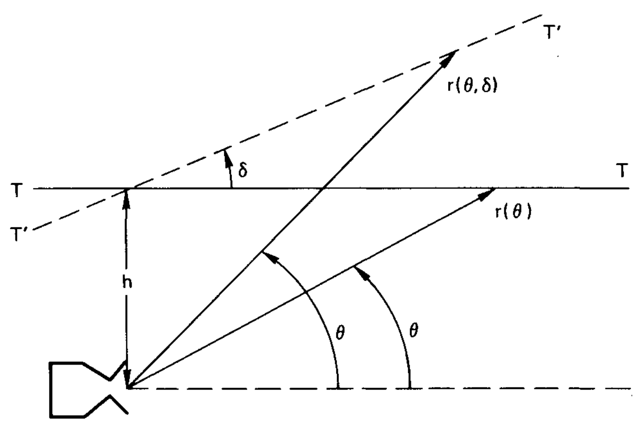

Fig. 2 Impingement coordinates on plane TT at $r = h/\sin\theta$ and on canted plane T′T′ at $r(\theta,\delta) = h\cos\delta/\sin(\theta-\delta)$.

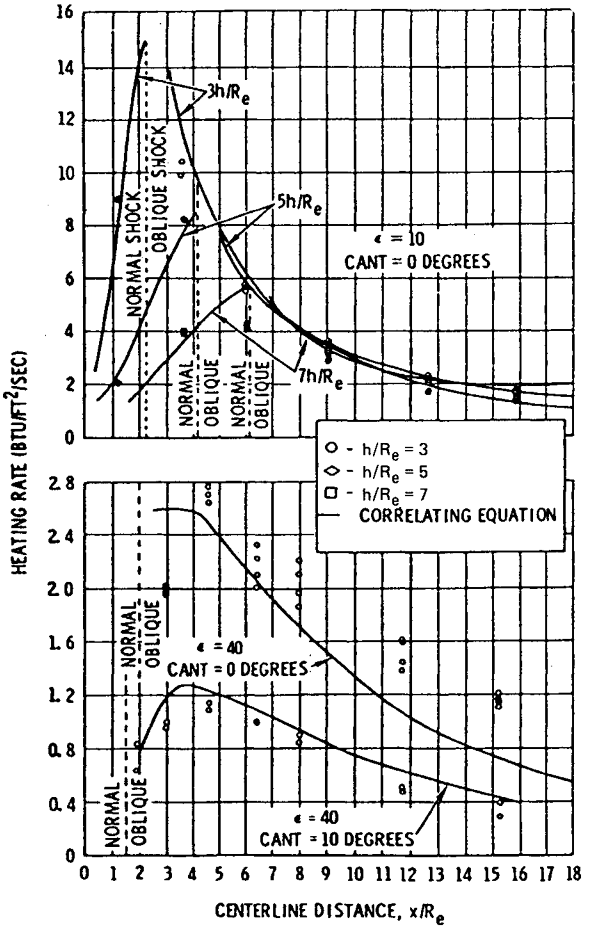

Fig. 3 Heating rate data and correlations adapted from Fig. 15 of Ref. 1.

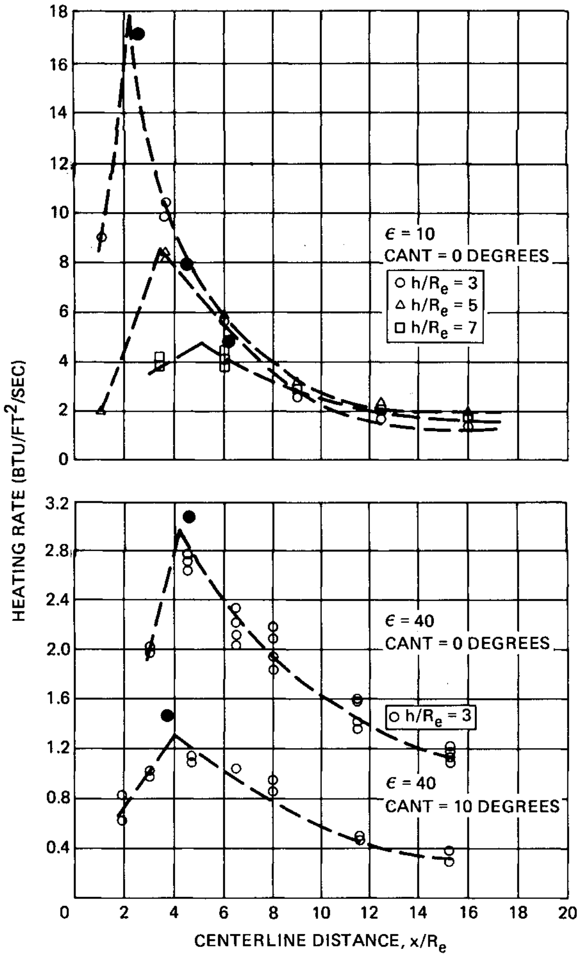

Fig. 4 Test data from Ref. 1 and calculated q_m in solid circles (●).

Table 1 Nozzle parameters

Expansion ratio ϵ	Throat radius R_t, in.	Exit radius R_e, in.	Exit angle θ_e, deg	Specific heat ratio γ
10	0.434	1.372	22.0	1.25
40	0.434	2.73	8.3	1.30

The influence of cant angle δ in Eqs. (12) and (13) is included in the subsequent derivations.

The location of the impact point at r_m is considered to be a stagnation point within the compressed Newtonian shock layer on the target plane. In the neighborhood of r_m, the pressure diminishes depending on the divergence of the plume velocity vector incident on the plane. The divergent incidence on the plane surface is analogous to the varying incidence of parallel streamlines on a spherical surface (re-entry vehicle nose of radius R_N) of general interest in hypersonic flow investigations employing Newtonian impact concepts. A particular result of such investigations[8] is the relationship between the radius R_N and the local velocity gradient at the freestream/shock-layer interface (du/dx') of the stagnation point,

$$\left(\frac{du}{dx'}\right)_s = \frac{\sqrt{2p_s/\rho_s}}{R_N} \tag{14}$$

where p_s and ρ_s refer to pressure and density, respectively, in the shock layer, u is the interface gas velocity, and x' is along the (spherical) surface. By analogy with (Eq. (14), the interface velocity of the diverging plume streamlines at the plane surface can be related to an effective radius R_p, which defines the high-pressure region in the neighborhood of the stagnation point,

$$\frac{d[V_\infty \cos(\theta-\delta)]}{d[x/\cos\delta]} = \frac{\sqrt{2p_m/\rho_m}}{R_p} \tag{15}$$

By use of the Newtonian pressure

$$p_m = \rho(\theta_m) V_\infty^2 \sin^2(\theta_m - \delta) \tag{16}$$

and of the compression ratio ρ_m/ρ in the limit of high velocity impact (Mach$\rightarrow\infty$),

$$\frac{\rho_m}{\rho} \rightarrow \frac{\gamma+1}{\gamma-1} \tag{17}$$

the following expression for R_p is obtained from Eq. (15):

$$R_p = \frac{h\cos\delta}{\sin^2(\theta_m-\delta)}\sqrt{\frac{2(\gamma-1)}{\gamma+1}} \tag{18}$$

This expression will be useful in defining an equivalent blunt-body radius R_b analogous to the spherical nose radius R_N required in calculation of the stagnation heat transfer during atmospheric re-entry.[5]

IV. Maximum Heat Flux

For the analysis of test data the peak heat flux calculation is based on a well-known atmospheric entry heating formula, appropriately modified for the geometry of plume impact in the test configuration. A convenient expression for the stagnation point heat flux[5] on the hemispheric nose of the re-entry body at initial temperature $T_i \cong 540°R$ is

$$q_N = \frac{865}{\sqrt{R_N}} \left(\frac{V_\infty}{10^4}\right)^{3.15} \sqrt{\frac{\rho}{\rho_{SL}}} \tag{19}$$

where q is in Btu/ft$^2\cdot$s, R_N in ft, V_∞ in ft/s, and ρ_{SL} designates sea level density (0.076 lb/ft^3).

If $T_i \neq 540°R$, q_N is calculated by multiplying the right-hand side of Eq. (19) by the factor $(T_g - T_i)/(T_g - 540)$, where T_g is the gas stagnation temperature. The adjustment factor is also valid for Eq. (21).

In adapting Eq. (19) to the stagnation point on the plane, two elementary modifications are required to account for 1) the geometry of the plume incidence and 2) the effective blunt-body radius R_b, which is analogous to the nose radius R_N in Eq. (19). The first of these is apparent by noting that the approximate third power of V_∞ arises from the transport of kinetic energy $V_\infty^2/2$ with impact speed V_∞. Accordingly, a $\sin(\theta_m - \delta)$ factor is introduced in Eq. (19) to account for the velocity component which represents the transport rate normal to the plane. Furthermore, as noted in the previous sections, a blunt-body radius R_b can be defined in proportion to the effective stagnation zone radius R_p in Eq. (18),

$$R_b = K^2 R_p \tag{20}$$

where K is an empirical factor to be determined by comparison of calculated values and observed data. With these modifications, Eq. (19) is converted to an expression for the maximum heat flux,

$$q_m = \frac{865 \sin^2(\theta_m - \delta)}{K\sqrt{(2(\gamma-1)/(\gamma+1)^{1/2} h \cos\delta}} \left(\frac{V_m}{10^4}\right)^{3.15} \sqrt{\frac{\rho(\theta_m)}{\rho_{SL}}} \tag{21}$$

where the density ratio, using Eqs. (1) and (13), becomes

$$\frac{\rho(\theta_m)}{\rho_{SL}} = \left(\frac{\beta+2}{8\pi}\right) \frac{\dot{W} \sin^2(\theta_m - \delta)}{V_\infty (h \cos\delta)^2 \rho_{SL}} \left(\cos\frac{\theta_m}{2}\right)^\beta \tag{22}$$

The comparison of q_m in Eq. (21) with test data on the maximum heat flux q_{max}, as detailed in the next section, leads to satisfactory agreement

$$q_m / q_{max} \approx 1 \pm 20\% \tag{23}$$

where the correlation parameter $K(=1.37)$ has been determined by minimizing the percent error between q_m and q_{max}.

V. Comparison with Test Data

Test Configuration and Heat Flux Data

The liquid rocket plume test data available for comparison with q_m were obtained in simulated high-altitude plume impingement tests.[1] Storable propellant rocket exhaust plumes were made to impinge on an instrumented flat plate placed at various angles and distances from the rocket exit, as shown in Fig. 2. The test parameter values specified in Ref. 1, required in the plume description, are a nominal total flow rate $\dot{W}$ of 0.33 lb/s of N_2O_4 oxidizer and 50% UDMH/50% N_2H_4 fuel (O/F ratio of 2) and the exit nozzle parameter values cited in Table 1. The γ values shown in the table have been computed for shifting equilibrium in the supersonic nozzle. An additional datum[9] is the limit speed $V_\infty = 1.01 \times 10^4$ ft/s for the O/F ratio of 2.

Table 2 Calculated and observed data comparison

ϵ	β	δ, deg	h/r_e, in.	θ_m, deg	θ_{max}, deg	q, Btu/ft$^2\cdot$s: $Q_m = Kq_m$	q_m	q_{max}
10	15.5	0	3	48.6	50.2[a]	23.2	16.9	18.0[a]
		0	5	48.6	55.0[b]	10.8	7.9	8.5[b]
		0	7	48.6	54.5	6.5	4.8	5.0
40	40	0	3	33.5	35.5	4.2	3.1	3.0
		10	3	39.9	36.8	2.1	1.5	1.3

[a]Ref. 1, Fig. 11. [b]Interpolated.

The reported heat flux test data, with the correlation proposed in Ref. 1, are shown here in Fig. 3 for the impingement configurations defined by three plate distance values ($h/R_e = 3$, 5, and 7) and two inclinations ($\delta = 0$ and 10 deg). It is evident from Fig. 3 that the peak heat flux q_{max} values can be obtained, in general, only by interpolation of the data obtained at the fixed positions of the thermocouples in the instrumented plate. When the test data in Fig. 3 are replotted as shown in Fig. 4, the interpolated q_{max} is obtainable from the dashed curves shown in the latter figure. (It is noted here that the q_{max} value of 18 Btu/ft$^2\cdot$s for $\epsilon = 10$ and $h/R_e = 3$ is also indicated in Fig. 11 of Ref. 1.) For comparison with q_{max}, Fig. 4 also shows the location and magnitude of q_m, calculated below.

Calculation of θ_m and q_m

From the above given values of rocket nozzle parameters ϵ, θ_e, and γ, the plume parameter β is calculated using Eqs. (5-7) and substituted into Eq. (11) to yield θ_m. With β and θ_m determined in this manner, the data on $\dot{W}$, V_∞, h, and δ used in Eqs. (21) and (22) enable the calculations of Kq_m designated by Q_m. Calculated results for comparison with test data θ_{max} and q_{max} are summarized in Table 2. In order to obtain the $q_m = Q_m/K$ data for comparison with q_{max}, the correlation parameter K is determined by minimizing the percent error, formulated as,

$$E^2 = \sum_{i=1}^{5} \left[\frac{q_{m,i} - q_{max,i}}{q_{max,i}}\right]^2 = \sum_{i=1}^{5} \left[\frac{Q_{m,i}/K}{q_{max,i}} - 1\right]^2 \tag{24}$$

The minimization of E^2 yields

$$K = \frac{\sum_{i=1}^{5} [Q_{m,i}/q_{max,i}]^2}{\sum_{i=1}^{5} [Q_{m,i}/q_{max,i}]} = 1.37 \tag{25}$$

which results in the listed values of q_m. The agreement between q_m and q_{max} obtained in this manner has been expressed in Eq. (23) and plotted in Fig. 4 at coordinate x_m/R_e defined by θ_m in the relation

$$\tan\theta_m = \frac{h/R_e}{x_m/R_e} + \tan\delta \tag{26}$$

VI. Conclusions

The principal steps in the analytic procedure developed for rapid estimation of peak heat-transfer rates due to plume impingement can be summarized as follows:

1) Calculate β from Eq. (5), using either analytically derived values of C_F and $C_{F,i}$, such as those obtainable from Eqs. (6) and (7), or test data on C_F, if available.

2) Calculate θ_m from Eq. (12).

3) Calculate V_∞ from thermal energy data consistent with energy release achieved in the combustion chamber (obtainable from c^* efficiency data).

4) For given plate configuration parameters h, δ, and total exhaust flow rate $\dot{W}$, calculate the density ratio $\rho(\theta_m)/\rho_{SL}$ in Eq. (22).

5) Finally, calculate q_m by substituting the preceding data into Eq. (21), using the value $K=1.37$ for the correlation constant.

The agreement obtained between calculated values of θ_m and q_m and the test data on θ_{max} and q_{max} cited in Table 2 supports the use of the procedure in preliminary design calculations involving propulsion system configuration tradeoff studies. Applicability of the procedure is limited to energetic liquid propellants, as inferred from the low-speed limit ($V_\infty \simeq 6000$ ft/s) of the re-entry heating equation (19).[5]

A preliminary attempt has been made to use the above procedure for analysis of the solid-propellant plume heat-transfer data of Ref. 2, obtained in tests of Centaur retrorocket plume impingement on a flat plate. No definite conclusions can be drawn because of the unavailability of the needed motor parameters and the uncertainties of solid-particle radiation effects reported for the 2% particle content of the propellants.

Appendix

From the source flow description of far-field density $\rho(r,\theta)$ in Eq. (1), the total mass flow rate $\dot{W}$ and thrust F can be expressed using conservation laws as

$$\dot{W}=2\pi V_\infty \int_0^\pi (\rho r^2)\sin\theta d\theta = 2\pi\alpha \int_0^\pi \left(\cos\frac{\theta}{2}\right)^\beta \sin\theta d\theta \quad \text{(A1)}$$

$$F=2\pi\frac{V_\infty^2}{g}\int_0^\pi \rho r^2 \sin\theta \cos\theta d\theta$$

$$=2\pi\frac{V_\infty}{g}\alpha\int_0^\pi \left(\cos\frac{\theta}{2}\right)^\beta \sin\theta \cos\theta d\theta \quad \text{(A2)}$$

In Eq. (A2) the thrust has been expressed as the reaction of the momentum flow in the axisymmetric far field. Evaluation of the integrals yields

$$\dot{W}=\frac{8\pi\alpha}{\beta+2} \quad \text{(A3)}$$

$$F=\frac{8\pi\alpha\beta V_\infty}{(\beta+2)(\beta+4)}=\frac{\beta}{\beta+4}\dot{W}\frac{V_\infty}{g} \quad \text{(A4)}$$

References

[1]Piesik, E.T., Koppang, R.R., and Simkin, D.J., "Rocket Exhaust Impingement on Flat Plate at High Vacuum," *Journal of Spacecraft and Rockets,* Vol. 3, Nov. 1966, pp. 1650–1657.

[2]Rochelle, W.C. and Kooker, D.E., "Heat Transfer and Pressure Analysis of Rocket Exhaust Impingement on Flat Plates and Curved Panels," *Journal of Spacecraft and Rockets,* Vol. 6, March 1969, pp. 718–724.

[3]Maddox, A.R., "Impingement of Underexpanded Plumes on Adjacent Surfaces," *Journal of Spacecraft and Rockets,* Vol 5, June 1968, pp. 718–724.

[4]Mayer, E., Hermel, J., and Rogers, A.W., "Thrust Loss Due to Plume Impingement Effects," Journal of Spacecraft and Rockets, Vol. 23, Nov.-Dec. 1986, pp. 554–560.

[5]Detra, R.W. and Hidalgo, H., "Generalized Heat Transfer Formulas and Graphs for Nose Cone Reentry Into Atmosphere," *Journal of the American Rocket Society,* Vol. 31, 1961, pp. 318–321.

[6]Sutton, G.P. and Ross, D.M., *Rocket Propulsion Elements,* Wiley, New York, 1976.

[7]Hayes, W.D. and Probstein, F.R., *Hypersonic Flow Theory,* Academic Press, New York, 1959.

[8]Rose, P.H. and Stark, W.I., "Stagnation Point Heat Transfer Measurements in Dissociated Air," *Journal of Aerospace Sciences,* Vol. 25, 1958, pp. 86–97.

[9]Ratliff, A.W., Audek, B.J., and Thornhill, D.D., "Analysis of Exhaust Plumes From Skylab—Configuration R-4D Attitude Control Motors," NASA CR-61332, March 1970.